

Power Loss Minimization of Permanent Magnet Synchronous Generator Using Particle Swarm Optimization

Prashant Kumar S. Chinamalli¹, Naveen T. S.², Shankar C. B.³

¹(Electrical Department, Yashoda Technical Campus/Shivaji University, India)

^{2,3}(Electrical & Electronics Department, Acharya Institute of Tecnology, Bangalore, Vishweshwaraih Technological University, India)

ABSTRACT: Interior Permanent-magnet synchronous generators (IPM) are commonly used for variable-speed wind turbines to produce high efficiency, high reliability, and low-cost wind power generation. An IPM driven by a wind turbine, in which the d -axis and q -axis stator-current components are optimally controlled to achieve the maximum wind power generation and Particle Swarm Optimization (PSO) for loss minimization of the IPMSG. The effect of magnetic saturation, which causes the highly nonlinear characteristics of the IPMSG, has been considered in the control scheme design. The optimal d -axis stator-current command is obtained as a function of the IPMSG rotor speed by solving a constrained nonlinear-optimization problem that minimizes the copper and core losses of the IPMSG. At any wind speed within the operating range, the IPMSG rotor speed is optimally controlled to extract maximum wind power. The PSO technique guides to narrow convergence solution of non-linearity introduced in the model. The proposed control scheme provides the wind generation system with the maximum efficiency and high dynamic performance [1] [2].

Keywords: Permanent magnet synchronous generator, magnetic saturation, loss minimization.

I. INTRODUCTION

Resolving the world's growing demand for energy, for minimizing related impacts on the environment and with increased competition for energy supplies represent some of the greatest technical challenges of the next several decades. Fossil fuels supply more than 80 percent of the world's primary energy but they are finite resources and major contributors to global climate change. The ways and means for their ultimate replacement with clean, affordable and sustainable energy sources at the scale required to power the world are not yet readily available. Turning off the carbon emissions is the first step and many of the solutions which are familiar are windmills, solar panels, nuclear plants etc... All three technologies are part of the energy mix, although each has its issues, including noise from windmills and radioactive waste from nukes. Moreover, existing energy infrastructures around the world are complex and large, where they require enormous capital investment and have operational Life spans of 50 years or more. In windmills (a much older technology) wind energy is used to turn mechanical machinery to do physical work; historically, windmills were used traditionally for grinding grain or spices, pumping water, sawing wood or hammering seeds. The evolution of modern turbines is a remarkable success story of engineering and scientific skill, coupled with a

Strong entrepreneurial spirit. The progress of wind energy around the world in recent years has been

consistently impressive with the main engineering challenge to the wind industry to design an efficient wind turbine to harness energy and turn it into electricity.

The use of permanent-magnet synchronous machines (PMSMs) for wind power generation has received increasing attention in recent years [1]–[6]. The PMSMs can provide high-efficiency and high-reliability power generation, since there is no need for external excitation and no copper losses in the rotor circuits. In addition, the high-power density PMSMs are small in size, which reduces the cost and weight of wind turbines. Furthermore, in the wind generation system equipped with a PMSM and power-electronic converters, the wind turbine can be operated to extract the maximum power from the wind at various wind speeds by adjusting the shaft speed optimally. Therefore, the PMSMs are commonly used for small variable-speed wind turbines to produce high efficiency, high reliability, and low-cost wind power generation.

Energy production and utilization, efficiency is always an important issue, so previously the minimization of the core losses of a PMSM through a suitable design of magnets and slots and the choice of the number of poles. In fact, the efficiency of an IPMSM can be improved not only during the machine design stage but also during the operation stage. By optimally controlling the d -axis component of the stator currents even by optimizing the values with particle swarm optimization, the stator copper and core losses of an IPMSM can be minimized.

II. MODELING OF WIND TURBINE SYSTEM

The basic configuration of an IPMSG driven by a wind turbine is as shown in Fig.1. The IPMSG converts the mechanical power from the wind turbine to ac electrical power, which is then converted to dc power through an IGBT pulse-width modulation (PWM) converter with a dc link to supply the dc load. Control of the IPMSG is achieved by controlling the ac-side voltages of this PWM power converter. By using an additional power inverter, the IPMSG can supply the ac electrical power with constant voltage and frequency to the power grid or ac load.

The mechanical power that the wind turbine extracts from the wind is calculated by

$$P_m = \frac{1}{2} \rho A_r v_w C_p(\lambda, \beta) \quad (1)$$

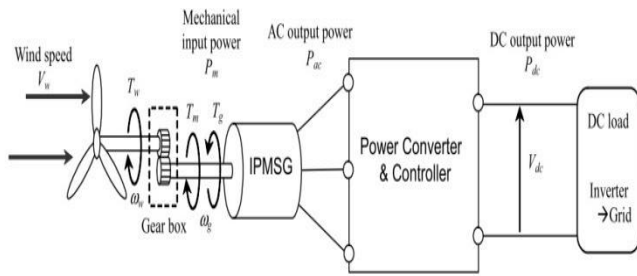


Fig. 1: Wind turbine system using IPMSG [4]

where ρ is the air density in kilograms per cubic meter, $A_r = \pi R^2$ is the area swept by the rotor blades in square meters, R is the wind-turbine rotor radius in meters, v_w is the wind speed in meters per second, and C_p is the power coefficient, which is a function of both tip-speed ratio λ and the blade pitch angle β . The mathematical representation of C_p is given by [4]

$$C_p(\lambda, \beta) = (0.3 - 0.00167\beta) \sin\left(\frac{\pi(\lambda + 0.1)}{10 - 0.3\beta}\right) - 0.000184(\lambda - 3)\beta(2)$$

Where λ is defined by $\omega_r R / v_w$ and ω_r is the wind-turbine rotational speed in radians per second.

The $C_p - \lambda$ curve described by Eqn (2) for the wind turbine is as shown in Fig. 2. In terms of Fig.2 and the definition of λ , at any wind speed within the operating range, there is a unique wind-turbine shaft rotational speed to achieve the maximum power coefficient C_{pmax} . In terms of Eqn (1), when C_p is controlled at the maximum value, the maximum mechanical power is extracted from the wind energy.

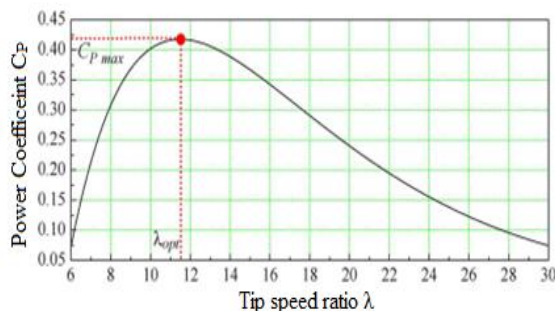


Fig. 2: $C_p - \lambda$ curve of the wind turbine.

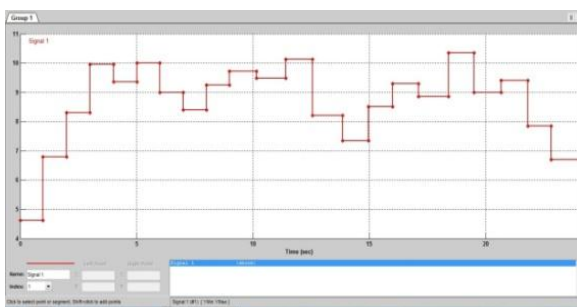


Fig. 3: Wind velocity input by signal builder.

The signal builder block is used to give wind speed as an input to the wind turbine which is as shown in Fig.3.

Wind speed is in the range of 4–11 m/s. The parameters of the wind turbine system as listed in Table. 1.

Table. 1: Parameters of the wind turbine system

Air density	1.08 kg/m ³
Rotor diameter	11 m
Rated wind speed	10 m/s
Rated rotational speed	200 m

III. MODELING OF PERMANENT MAGNET SYNCHRONOUS GENERATOR

Permanent Magnet Synchronous machines (PMSM's) are non-salient pole AC synchronous motors, these synchronous motor drives are suitable for constant speed applications as its speed of operation depends only on the frequency of the stator supply. Synchronous motor with permanent magnet is a choice in kW range for applications like wind turbines, aerospace actuators, electric vehicles etc. The advantages of permanent magnet synchronous motor over the other motors are of higher efficiency, higher torque to inertia ratio and compact in size. The PMSM used here is an Interior Permanent Magnet Synchronous Generator (IPMSG).

3.1 Dynamic Modeling:

The stator consists of three phase winding having spatial displacement from each other. The axis of phase-1 is taken as reference axis for the stationary co-ordinates fixed to the stator. The currents in the winding can have any general variation with respect to time. Assuming that the spatial distribution of mmf produced by each coil is sinusoidal in nature, the stator mmf caused by three phase currents flowing in the three windings can be represented by a single time varying quantity which has got some spatial orientation. The stator current space phasor diagram is shown in Fig. 4. The space vector of stator current can be represented in terms of three phase currents as,

$$i_s^s(t) = i_{s1}(t) + i_{s2}(t)e^{j\gamma} + i_{s3}(t)e^{j2\gamma} \quad (3)$$

where i_{s1}, i_{s2} and i_{s3} are the stator phase currents and γ is the advanced current angle.

The space vector of stator current can also be represented in terms of equivalent two phase ($\alpha - \beta$) axis currents as,

$$i_s^s(t) = i_{s\alpha}(t) + j i_{s\beta}(t) \quad (4)$$

As $\gamma = 120^\circ$, the α axis current and β axis currents can be written as,

$$i_{s\alpha}(t) = i_{s1}(t) \cos 0 + i_{s2}(t) \cos 120 + i_{s3}(t) \cos 240 \quad (5)$$

$$i_{s\beta}(t) = i_{s1}(t) \sin 0 + i_{s2}(t) \sin 120 + i_{s3}(t) \sin 240 \quad (6)$$

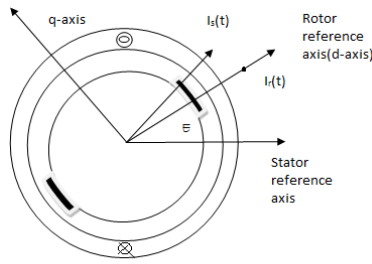


Fig.4: Representations of Co-ordinate Systems

The above equation can be simplified as,

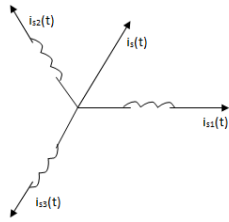


Fig.5: Stator current space phasor

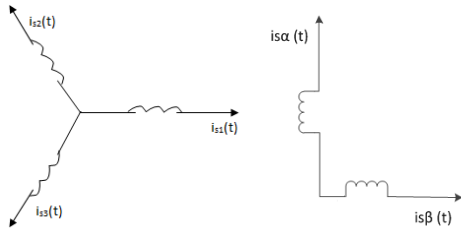


Fig.6: Stator current transformation from three phase to α-β axis.

$$i_{s\alpha}(t) = i_{s1}(t) - \frac{1}{2}i_{s2}(t) - \frac{1}{2}i_{s3}(t) \quad (7)$$

$$i_{s\beta}(t) = \frac{\sqrt{3}}{2}i_{s2}(t) - \frac{\sqrt{3}}{2}i_{s3}(t) \quad (8)$$

For a three phase wire system the condition,

$$i_{s1}(t) + i_{s2}(t) + i_{s3}(t) = 0 \quad (9)$$

holds good for all instants of time. Using this condition in above and (α-β) axis currents can be written as,

$$i_{s\alpha}(t) = \frac{3}{2}i_{s1}(t) \quad (10)$$

$$i_{s\beta}(t) = \frac{\sqrt{3}}{2}i_{s2}(t) - \frac{\sqrt{3}}{2}i_{s3}(t) \quad (11)$$

For the dynamic modeling, first convert the three quantities to two phase quantities i.e. abc to α-β transformation. The general formula can be given as below,

$$X_\alpha = \frac{3}{2}X_a \quad (12)$$

$$X_\beta = \frac{\sqrt{3}}{2}(X_b - X_c) \quad (13)$$

$$v_{s\alpha} = \frac{3}{2}v_{sa} \quad (14)$$

$$v_{s\beta} = \frac{\sqrt{3}}{2}(v_{sb} - v_{sc}) \quad (15)$$

Similarly the transformation of stator currents and voltages from α-β to d-q co-ordinates is done using the angle ε.

$$v_{sd} = v_{s\alpha} \cos \epsilon + v_{s\beta} \sin \epsilon \quad (16)$$

$$v_{sq} = v_{s\beta} \cos \epsilon - v_{s\alpha} \sin \epsilon \quad (17)$$

where ε is the angle between rotor reference axis and stator reference axis.

The above equations are used in the modeling of transformation of co-ordinates and sources as shown in the below Fig. 7, 8 and 9.

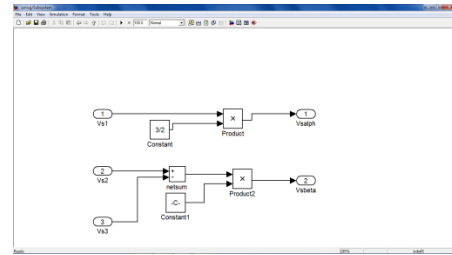


Fig.7: abc to α-β transformation

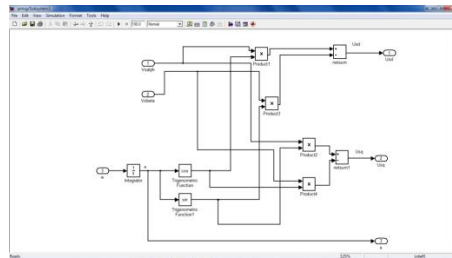


Fig.8: α-β to d-q transformation

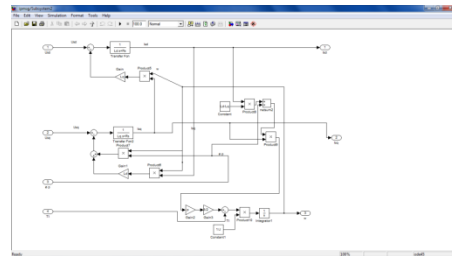


Fig.9: Voltage to Current transformation

3.2 Non-Linearity due to Magnetic Saturation:

Consider a typical Interior PMSG circuit as below in Fig.10. For the IPMSG, burying the magnets inside the rotor introduces saliency into the rotor into the rotor magnet circuit. The d-axis flux passes through a wide region of low-permeability magnets, while the q-axis flux path has a high permeability. Therefore, the IPMSG has a saliency ($L_q > L_d$) and the effect of magnetic saturation along the q-axis is dominant. Interior PMSG is considered with magnetic saturation, i.e. there is a flux linkage between the q-axis inductances so the L_q will be the function of current i_q and d-axis inductance L_d will be considered constant value and they are represented as $L_d, L_q(i_q)$. The dynamic equation of a three-phase IPMSG can be written in the rotor reference frame as.

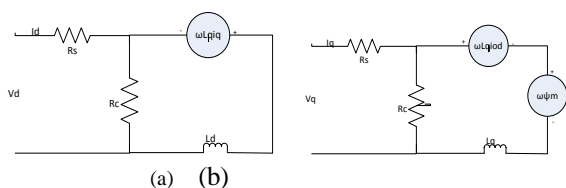


Fig.10. Equivalent circuits of the IPMSG. (a) d-axis equivalent circuit. (b) q-axis equivalent circuit.

$$L_d \frac{di_{od}}{dt} = -R_s i_d + \omega L_q(i_q) i_{oq} + v_d \quad (18)$$

$$L_q(i_q) \frac{di_{oq}}{dt} = -R_s i_q - \omega L_d i_{od} - \omega \psi_m + v_q \quad (19)$$

The electromagnetic torque developed by the machine is given by,

$$T_g = -\frac{3}{4} P_n [\psi_m i_{oq} + (L_d - L_q(i_q)) i_{od} i_{oq}] \quad (20)$$

The following equations help in complete dynamic modeling of IPMSG:

$$v_d = L_d \frac{di_{od}}{dt} + R_s i_d - \omega L_q(i_q) i_{oq} \quad (21)$$

$$v_q = L_q(i_q) \frac{di_{oq}}{dt} + R_s i_q + \omega L_d i_{od} + \omega \psi_m \quad (22)$$

$$J \frac{d\omega}{dt} = T_m - T_g \quad (23)$$

$$\omega = \int \frac{1}{J} (T_m - T_g) dt \quad (24)$$

$$\frac{d\epsilon}{dt} = \left(\frac{P}{2}\right) \omega = \omega_g \quad (25)$$

where ψ_m is the magnet flux linkage, R_s is the stator resistance, P_n is the number of poles, T_m is the input mechanical torque given by $T_m = P_m / \omega_g$, ω_g is the rotor speed, J is the inertia, i_{od} , i_{oq} are initial current values of d-axis and q-axis respectively, L_d is the d-axis inductance and assumed to be constant, and L_q is the q-axis inductance which varies depending on the value of i_q .

The effect of magnetic saturation is considered by modeling L_q as a function of i_q given by [1],

$$L_q = L_{q0} - k |i_q| \quad (26)$$

where k is a positive constant, the parameters of the IPMSG are given in the Table 2.

All the above equations along with parameters specified in Table.2 are used to model interior permanent magnet synchronous generator considering magnetic saturation as shown below in Fig.11.

Table 2. Parameters of IPMSG

R_s	0.1764 Ω
L_d	6.24 mH
L_{q0}	20.5822 mH
ψ_m	0.246 Wb
J	1.2 kg . m ²
P_n	6
k	0.1879 mH/A

Rated power	25 kW
Rated rotor speed	1200 rpm

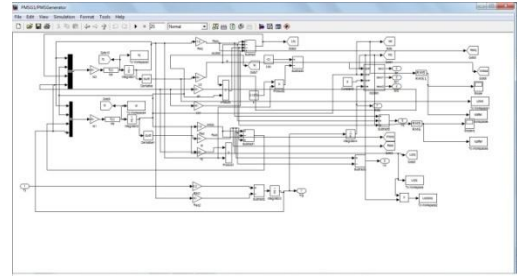


Fig 11. Simulink model of IPMSG

3.3 PWM Generator Side Converter:

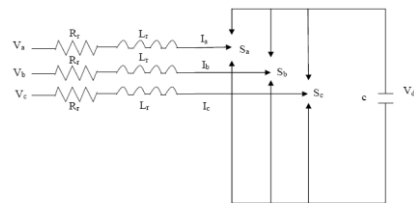


Fig . 12. PWM generator side converter

The pulse width modulation generator side converter consists of IGBT based 3-phase bridge voltage-source converter. The only difference between rectifier and inverter is the definition of power sign. The switching frequency of the converter is assumed to be sufficiently high to make an average analysis valid, which means that the switching ripple should be negligible compared to the averaged values. The generator side converter is shown in Fig. 12. The system equation for generator side converter can be written as:

$$V_a = R_r I_a + L_r \frac{dI_a}{dt} + V_{dc} \cdot \frac{2S_a - S_b - S_c}{3} \quad (27)$$

$$V_b = R_r I_b + L_r \frac{dI_b}{dt} + V_{dc} \cdot \frac{-S_a + 2S_b - S_c}{3} \quad (28)$$

$$V_c = R_r I_c + L_r \frac{dI_c}{dt} + V_{dc} \cdot \frac{-S_a - S_b + 2S_c}{3} \quad (29)$$

where V_a, V_b, V_c are the three phase stator voltage; I_a, I_b, I_c are three phase currents; S_a, S_b, S_c are gate pulses to IGBT and V_{dc} is DC link voltage.

IV. MODELING FOR MAXIMUM WIND POWER GENERATION WITH LOSS MINIMIZATION

4.1 Maximum Wind Power Generation:

By adjusting the wind-turbine shaft speed optimally, the tip speed ratio λ can be controlled at the optimal value to achieve the maximum power coefficient C_{Pmax} regardless of the wind speed. The maximum mechanical power is therefore extracted from the wind energy. At this optimal condition, the optimal IPMSG rotor speed is proportional to the wind speed, given by

$$\omega_{g,opt} = k_\omega v_w \quad (30)$$

Where k_ω is a constant determined by the wind-turbine characteristics. The generator rotor speed must be a nearer

value to the optimal rotor speed which leads to the extraction of maximum power from wind velocity.

4.2 Minimization of the Copper and Core Losses of IPMSG:

The losses of a PMSG can be decomposed into four components, namely, stator copper loss, core loss, mechanical loss, and stray-load loss. Only the stator copper and core losses are explicitly dependent on and can be controlled by the fundamental components of the stator currents. Therefore, the maximum efficiency condition of the IPMSG is obtained by solving the following nonlinear-optimization problem offline to minimize the total copper and core losses of the IPMSG

i.e we have

$$P_{loss} = P_{copper} + P_{core} \quad (31)$$

$$P_{copper} = 1.5 R_s (i_d^2 + i_q^2) \quad (32)$$

$$P_{core} = 1.5 (i_{cd}^2 + i_{cq}^2) R_c (\omega_g) \quad (33)$$

$$= 1.5 \omega_g^2 \frac{[(L_d i_{od} + \psi_m)^2 + (L_q (i_q) i_{oq})^2]}{R_c (\omega_g)} \quad (34)$$

Where P_{copper} is the copper loss, P_{core} is the core loss [6], and i_{cd} and i_{cq} are the currents at the resistant R_c .

An optimal IPMSG rotor speed calculated by Eqn (30), the solutions of the nonlinear-optimization problem yield the optimal values of i_d and i_q , which minimize the total copper and core losses of the IPMSG. Therefore, at any wind speed, the solutions of Eqn (30) and Eqn (34) provide the desired optimal IPMSG rotor speed, optimal currents i_d and i_q to achieve the maximum wind power extraction, and loss minimization of the IPMSG. Without considering the effect of magnetic saturation (i.e., L_q is constant) and the variation of R_c , Eqn (34) would be a constrained nonlinear quadric optimization problem that can be solved by conventional nonlinear-optimization methods. However, the inclusion of magnetic saturation and variation of R_c results in a complex nonlinear-optimization problem that requires extensive computation effort when using conventional nonlinear optimization methods. In order to achieve this stochastic optimization technique called particle swarm optimization (PSO) [5] is employed to obtain the optimal solution of Eqn (34).

V. PARTICLE SWARM OPTIMIZATION

Particle Swarm Optimization is a population-based stochastic optimization technique. It searches for the optimal solution from a population of moving particles. Each particle represents a potential solution and has a position (vector x_i) and a velocity (vector v_i) in the problem space. Each particle keeps track of its individual best position $x_{i,pbest}$, which is associated with the best fitness it has achieved so far, at any step in the solution. Moreover, the best position among all the particles obtained so far in the swarm is kept track of as x_{gbest} . This information is shared by all particles.

The PSO algorithm is implemented in the following iterative procedure to search for the optimal solution.

- 1) Initialize a population of particles with random positions and velocities of M dimensions in the problem space.
- 2) Define a fitness-measure function to evaluate the performance of each particle.
- 3) Compare each particle's present position x_i with its $x_{i,pbest}$ based on the fitness evaluation. If the current position x_i is better than $x_{i,pbest}$, then set $x_{i,pbest} = x_i$.
- 4) If $x_{i,pbest}$ is updated, then compare each particle's $x_{i,pbest}$ with the swarm best position x_{gbest} based on the fitness evaluation. If $x_{i,pbest}$ is better than x_{gbest} , then set $x_{gbest} = x_{i,pbest}$.
- 5) At iteration k , the velocity of each particle is updated by

$$v_i(k+1) = w \cdot v_i(k) + c_1 \phi_1 (x_{i,pbest}(k) - x_i(k)) + c_2 \phi_2 (x_{gbest}(k) - x_i(k)), \quad i=1, 2, \dots, N. \quad (35)$$

- 6) Based on the updated velocity, each particle then changes its position by
- $$x_i(k+1) = x_i(k) + v_i(k+1), \quad i=1, 2, \dots, N. \quad (36)$$
- 7) Repeat steps (3) to (6) until a criterion, usually a sufficiently good fitness or a maximum number of iterations, is achieved.

The final value of x_{gbest} is regarded as the optimal solution of the problem.

In Eqn (35), c_1 and c_2 are positive constants representing the weighting of the acceleration terms that guide each particle toward the individual best and the swarm best positions, $x_{i,pbest}$ and x_{gbest} , respectively; ϕ_1 and ϕ_2 are uniformly distributed random numbers in $[0, 1]$; w is a positive inertia weight developed to provide better control between exploration and exploitation; N is the number of particles in the swarm. The last two terms in Eqn (12) enable each particle to perform a local search around its individual best position $x_{i,pbest}$ and the swarm best position x_{gbest} . The first term in Eqn (35) enables each particle to perform a global search by exploring a new search space.

Because of many attractive features, e.g., multi-agent search, simple implementation, small computational load, and fast convergence, the PSO algorithm can provide a fast and efficient search for the optimal solution. These features provide PSO with superior performance over other evolutionary computation algorithms (e.g., genetic algorithms) in many applications. In addition, for many complex optimization problems that are difficult to formulate mathematically or to solve by traditional optimization methods, PSO is efficient to find the optimal solution.

The values of the PSO parameters are chosen as:

$$c_1 = c_2 = 2, \quad N = 20 \quad \text{and} \quad w = 1.4 - (1.4 - 0.4)$$

$*(k/K)$, where k is the iteration number and K is the maximum number of iterations. The PSO algorithm only performs a 1-D search for the optimal value of i_q . The optimal value of i_d is determined by the torque in Eqn (20) and the corresponding optimal value of i_q , where the electrical torque T_g in Eqn (20) is determined by Eqn (30) and the constraint equations of Eqn (34). The fitness-measure function is simply the total copper and core losses P_{loss} of the IPMSG. It is calculated by the first two constraint equations of Eqn (34). By solving the nonlinear-optimization problem in Eqn (34) at various IPMSG rotor speeds, the optimal values of i_d and i_q are obtained as functions of the IPMSG rotor speed ω_g . The relationship between the optimal d -axis and q -axis stator-current

components and the IPMSG rotor speed can be approximated by a fourth-order and a third-order polynomial, respectively, given by

$$i_{d,opt} = K_{d4}\omega_g^4 + K_{d3}\omega_g^3 + K_{d2}\omega_g^2 + K_{d1}\omega_g + K_{d0} \quad (37)$$

$$i_{q,opt} = K_{q3}\omega_g^3 + K_{q2}\omega_g^2 + K_{q1}\omega_g + K_{q0} \quad (38)$$

The coefficients of both polynomials are listed in Table 3. However, it should be pointed out that Eqn (37) and Eqn (38) only provide the optimal operating conditions of the IPMSG for the wind speed below the rated value. When the wind speed exceeds the rated value, the phase current and/or the terminal voltage reach their ceiling values, and therefore, the optimal speed tracking control cannot be applied. Under this condition, the current and voltage limited maximum output control can be applied to control IPMSG.

Table 3. Coefficients of approximating polynomials

Coefficients of $i_{d,opt}$		Coefficients of $i_{q,opt}$	
K_{d4}	1.291×10^{-11}	K_{q3}	7.528×10^{-9}
K_{d3}	-3.523×10^{-8}	K_{q2}	-3.477×10^{-5}
K_{d2}	1.154×10^{-5}	K_{q1}	-1.648×10^{-3}
K_{d1}	-1.348×10^{-2}	K_{q0}	1.263
K_{d0}	-1.589×10^{-2}		

VI. CONTROL OF PMSG

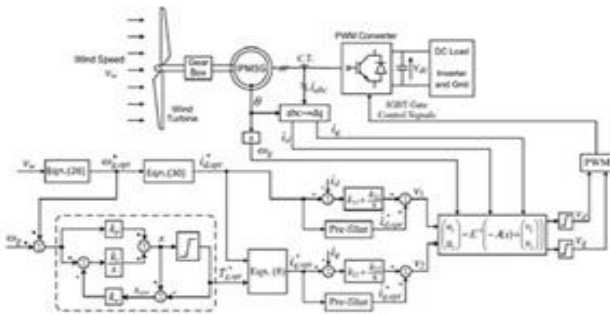


Fig. 13: Control of scheme for the IPMSG

6.1 Optimal IPMSG Rotor-Speed Tracking Control:

Based on the IPMSG motion Eqn (23), a PI-type speed controller is designed to track the optimal rotor speed at any moment, applied for the speed controller, as shown by the dash-line block in Fig. 22. The gain k_a is given by $k_a = 1/k_p$. The output of the speed controller is the optimal torque command $T_{g,opt}^*$ for the IPMSG, which corresponds to the maximum power point for wind power generation. By using this optimal torque command and the optimal d-axis current command from Eqn (37), the solution of Eqn (20) provides the optimal q-axis stator-current command for the inner loop current regulation. In the real application, the values of $i_{q,opt}^*$ can be generated offline over the entire operating range of the IPMSG.

6.2 IOL- Based Non-Linear Current Control:

Instead of approximating a nonlinear system's dynamics locally around some operating point via linearization, the IOL technique transforms the nonlinear system into an equivalent linear system via feedback and nonlinear coordinate transformation. This is a systematic way to globally linearize a part of or all the dynamics of the nonlinear system. In such a scheme, the input-output dynamics are linearized, but the state equations may be only partially linearized. Residual nonlinear dynamics, called internal dynamics, do not depend explicitly on the system input and, thus, are not controlled. If the internal dynamics are trivial or stable at the equilibrium point, then the entire nonlinear system can be stabilized by a standard linear feedback control using the linearized input-output dynamics.

VII. RESULTS

The model of Wind turbine system and IPMSG are previously run for the existing condition of initial values. Later, speed control and current control techniques are introduced for the optimization of rotor speed and current by running Particle Swarm Optimization algorithm. In PSO algorithm the complete model is called through command to get the desired output of Maximum generation and Power loss minimization. All results are taken from the simulation of the modeling in MATLAB 2011b.

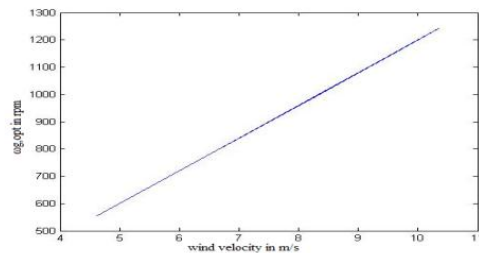


Fig .14. wind velocity Vs $\omega_{g,opt}$

As per the Eqn(30) the $\omega_{g,opt}$ varies linearly with respect to the wind velocity as shown in Fig .14. From this it can be justified that as the wind velocity varies the rotor speed varies optimally in a linear manner.

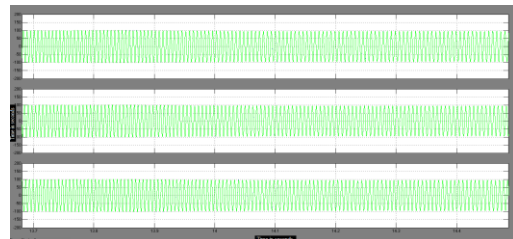


Fig. 15. Three phase stator current

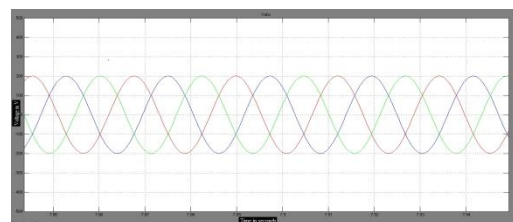


Fig .16. Three stator voltage

Fig. 15 and Fig. 16 show the three-phase controlled stator current and voltage of the IPMSG after PSO. As voltage is 200V and current is 100A so it can be stated that WTG system generates upto 20 Kw power. The simulated result for a dc link current, which is controlled by the rectifier side controller, is as shown in Fig. 17.

For maximum wind power tracking the speed controller is employed, this can be noticed from Fig 18 and Fig 19. Because of the relatively slow response of the WTG mechanical system, during the acceleration of the WTG, the PI-type speed controller is saturated, and the resulting IPMSG electrical-torque command generated by the speed controller remains at its limit value of zero.

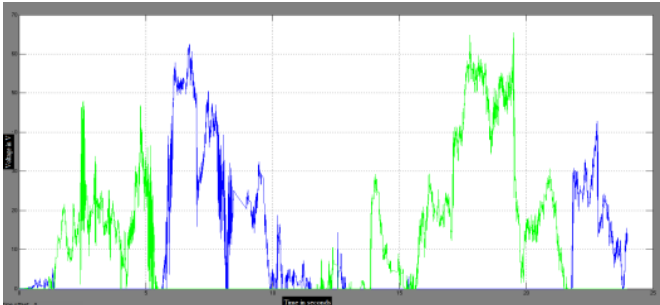


Fig .17. DC link voltage

As a result, the electrical output power and the *q*-axis stator current of the IPMSG are both regulated at zero during the saturation of the speed controller.

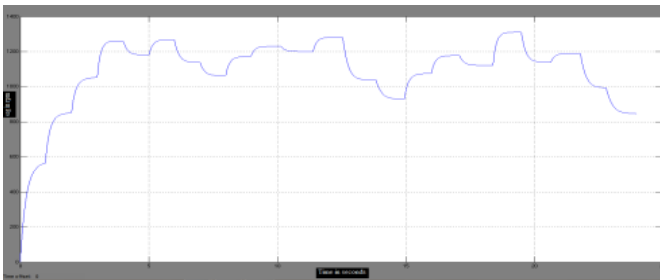


Fig .18. Time Vs ω_g

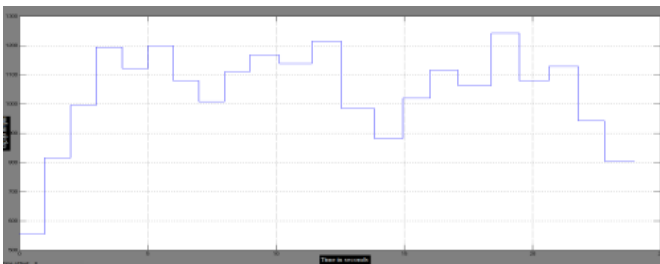


Fig. 19. Time Vs $\omega_{g,opt}$

The optimized results of current of d-axis and q-axis are shown Fig. 20 and Fig. 21. It can be observed that by the optimization the magnetic saturation is nullified.

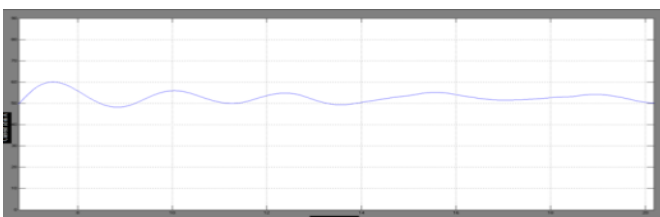


Fig .20. Time Vs I_d , after PSO

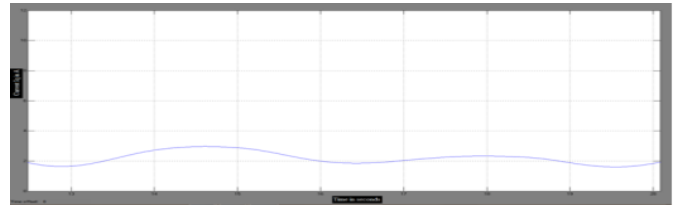


Fig. 21. Time Vs I_q , after PSO

After the PSO algorithm the optimized results of currents are incorporated in Eqn (34), hence there is a minimization in the total power loss as shown in Table 5.

Table .5. Total P_{loss} minimization

Total P_{loss} before PSO	Total P_{loss} after PSO	Total P_{loss} minimization
3.3 kW	2.57 kW	22.12%

VIII. CONCLUSION

Modeling and simulation of a 25kW variable speed wind energy conversion system employing a Maximum Torque per Current control and Particle Swarm Optimization is presented in the paper. PMSGs are commonly used for small variable speed WTG systems. In such systems, by adjusting the shaft speed optimally, the maximum wind power can be extracted at various wind speeds within the operating range. In addition, when using an IPMSG, the stator copper and core losses of the generator can be minimized by optimally controlling the *d*-axis component of the stator currents. However, to achieve the high performance of the WTG system, magnetic saturation of the IPMSG must be taken into account in the control-system design. Implementation of PSO results in the minimization of total power loss and thus improves the efficiency of the system. This proposed control provides the wind generation system with high dynamic performance and improved power efficiency.

REFERENCES

- [1] T. M. Jahns, G. B. Kliman, and T. W. Neumann, "Interior permanentmagnetsynchronous motors for adjustable-speed drives," *IEEE Trans. Ind. Appl.*, vol. IA-22, no. 4, pp. 738–747, Jul./Aug. 1986.
- [2] E. Muljadi, C. P. Butterfield, and Y. Wang, "Axial-flux modular permanent- magnet generator with a toroidal winding for wind-turbine applications," *IEEE Trans. Ind. Appl.*, vol. 35, no. 4, pp. 831–836, Jul./Aug. 1999.
- [3] S. Grabic, N. Celanovic, and V. A. Katic, "Permanent magnet synchronous generator for wind turbine application," *IEEE Trans. Power Electron.*, vol. 13, no.3, pp. 1136–1142, May 2008.
- [4] S. Morimoto, H. Nakayama, M. Sanada, and Y. Takeda, "Sensorless output maximization control for variable-speed wind generation system using IPMSG," *IEEE Trans. Ind. Appl.*, vol. 41, no. 1, pp. 60–67, Jan./Feb. 2005.
- [5] Y. Shi and R. C. Eberhart, "Empirical study of particle swarm optimization," in *Proc. IEEE Int. Conf. Evol. Comput.*, May 4–9, 1998, pp. 69–73
- [6] H. Li, Z. Chen, Institute of Energy Technology, Aalborg University, Aalborg East DK-9220, Denmark, "Overview of different wind generator systems and their comparisons". Published in *IET Renewable Power Generation* Received on 24th January 2007, Revised on 23rd August 2007.

BIOGRAPHY

Prashantkumar.S.Chinamalli born in Shahapur, Karnataka, India on 10th June 1987, received his B.E. degree in Electrical & Electronics Engineering department from Poojya Doddappa Engineering College, Gulbarga in 2010. M.Tech in Power & Energy System from Basaveshwara Engineering Department in 2012. His areas of interest include Power System, Drives and Renewable Energy Sources. He is presently working as Asst. Prof in the Department of Electrical Engineering at Yashoda Technical Campus/Shivaji University, Pune, India.

Naveen T S born in Bangalore, Karnataka, India on 11th Oct 1986, received his B.E. degree in Electrical & Electronics Engineering department from Acharya Institute of Technology, Bangalore in 2008. M.Tech in Power & Energy System from Basaveshwara Engineering Department in 2012. His areas of interest include Power System, Reactive Power management. He is presently working as faculty in the Department of Electrical & Electronics Engineering at Acharya Institute of Technology, Bangalore, India.

Dr. Shankar C B was born in Raichur, Karnataka, India in 1969. He obtained B.E (Electrical & Electronics) and M.E. (Energy systems) degree from Karnataka University Dharwad, Karnataka, India in 1991 and Dec 94 respectively. He got his Ph D from VTU in 2011. His areas of interest include FACTS controllers, optimization techniques and intelligent systems.

He has attended National and International Conferences. He is member of IEEE and presently working as Professor in the Department of Electrical & Electronics Engineering at Acharya Institute of Technology, Bangalore, India.